Life Sciences 232 (2019) 116610

Contents lists available at ScienceDirect

Life Sciences

journal homepage: www.elsevier.com/locate/lifescie

The novel diterpene 7β-acetoxy-20-hydroxy-19,20-epoxyroyleanone from *Salvia corrugata* shows complex cytotoxic activities against human breast epithelial cells

Katia Cortese[a,*], Silvia Marconi[a], Carolina D'Alesio[b], Daniela Calzia[c], Isabella Panfoli[c], Sara Tavella[a,d], Cinzia Aiello[d], Francesca Pedrelli[c], Angela Bisio[c], Patrizio Castagnola[d]

[a] DIMES, Department of Experimental Medicine, Human Anatomy, University of Genoa, Genoa, Italy
[b] DiMI, Department of Internal Medicine and Medical Specialties, University of Genoa, Genoa, Italy
[c] DIFAR, Department of Pharmacy, University of Genoa, Genoa, Italy
[d] Department of Integrated Oncological Therapies, IRCCS Ospedale Policlinico San Martino, Genoa, Italy

ARTICLE INFO

Keywords:
Diterpenes
Breast
ERBB2
Mitochondria
ERK1/2
ROS

ABSTRACT

Aims: The aim of this study was the characterization of the in vitro cytotoxic properties of a recently isolated diterpene compound, 7β-acetoxy-20-hydroxy-19,20-epoxyroyleanone (compound 1), extracted from *Salvia corrugata*, versus human cell lines.

Main methods: We used as model study immortalized breast epithelial cells MCF10A and two ERBB2$^+$ breast cancer (BCa) cell lines, SKBR-3 and BT474. Compound 1 was isolated by methanolic extraction from regenerated shoots of *Salvia corrugata Vahl*, and purified by high pressure liquid chromatography (HPLC). Flow cytometry (FCM) was employed for cell cycle, apoptosis and reactive oxygen species (ROS) analysis. Cell morphology was assessed by immunofluorescence and transmission electron microscopy (TEM).

Key findings: Compound 1 inhibited cell survival of all breast cell lines. In particular, compound 1 promoted cell cycle arrest in the G0/G1 phase and apoptosis along with impairment of the mitochondrial function, which was reflected in a gross alteration of the mitochondrial network structure. Furthermore, we also detected a potent activation of the ERK1/2 kinase, which suggested the induction of reactive oxygen species (ROS). Partial rescue of survival obtained with *n*-acetylcysteine (NAC) when coadminstered with compound 1 further supported a contribution of ROS mediated mechanisms to the growth-arrest and proapoptotic activity of compound 1 in both BCa cell lines. ROS production was indeed confirmed in SKBR-3.

Significance: Our findings show that compound 1 has a cytotoxic activity against both human normal and cancer cell lines derived from breast epithelia, which is mediated by ROS generation and mitochondrial damage.

1. Introduction

Breast cancer (BCa) is one of the most common malignancies in women and the associated mortality is primarily due to the development of metastatic disease [1]. Progression of the disease involves the acquisition of adaptive changes within tumor cells and the tumor microenvironment. Nowadays, gene expression profiling has identified four main subtypes of breast cancer that differ in driver genes and optimal therapies [2,3]. The human epidermal growth factor receptor-2 (ERBB2)-positive (ERBB2$^+$) subtype, characterized by overexpression of ERBB2 receptor, represents up to 20% of cases and has high rates of metastases. Novel findings on the ERBB2$^+$ subtype have revealed that it has a distinctive transcriptional landscape that reflects androgen receptor signaling as replacement for estrogen receptor (ER)-driven tumorigenesis [4]. In addition to development of novel targeted drugs, the search for safer and effective chemoprevention for aggressive breast cancers would effectively help the management of this disease and lower the costs for cancer care [5]. Cancer chemoprevention with natural phytochemical compounds is an emerging strategy that aims to prevent and/or delay cancer progression.

A series of diterpenes and triterpenes, mainly obtained from genera of the Lamiaceae family have shown antineoplastic effects coupled with low toxicity profiles [6]. Recently, the effects of carnosic acid (CA), a diterpene obtained from various genera of Lamiaceae like *Salvia officinalis* L. and *Rosmarinus officinalis L.*, have been investigated in human glioblastoma and breast cancer cells [7,8]. This latter study reported, in

* Corresponding author at: DIMES, Dipartimento di Medicina Sperimentale, Anatomia Umana, Via Antonio de Toni 14, 16132 Genoa, Italy.
E-mail address: cortesek@unige.it (K. Cortese).

https://doi.org/10.1016/j.lfs.2019.116610
Received 27 March 2019; Received in revised form 25 June 2019; Accepted 26 June 2019
Available online 27 June 2019
0024-3205/

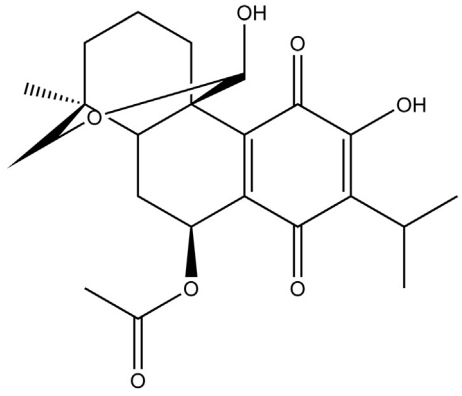

Fig. 1. Structural formula of compound 1.

particular, the potential benefit of the use of CA in the treatment of ERBB2$^+$ and Trastuzumab resistant BCa cell lines. However, many studies performed with the diterpenes did not evaluate the effects of these compounds on normal human cells, which is essential to determine a potential use in cancer therapy.

The 7β-acetoxy-20-hydroxy-19,20-epoxyroyleanone (7β-acetoxy-12,20-dihydroxy-19,20-epoxy-11,14-dioxoabieta-8,12-diene) (compound 1) is a diterpenoid extracted from regenerated shoots of *Salvia corrugata Vahl*, which structural formula is shown in Fig. 1. This compound showed weak antimicrobial activity against methicillin-resistant *Staphylococcus aureus* (MRSA), methicillin-resistant *Staphylococcus epidermidis* (MRSE) and vancomycin resistant *Enterococcus faecium* (VRE) [9]. The aim of this study was to characterize at the molecular level the cytotoxic effects of compound 1 on human ERBB2$^+$ breast cancer and normal breast epithelial cell lines to determine its potential use in cancer therapy.

2. Materials and methods

2.1. Compound 1 isolation

The methanolic extracts of regenerated shoots of *Salvia corrugata* Vahl (1.48 g) (b) were fractionated by Si gel MPLC (Merck Kiesegel 60, 230–400 mesh, 200 g) (Merck, Darmstadt, Germany) eluting with n-hexane/CHCl3/CH3OH at concentrations varying from 100:0:0 to 0:0:100 (a: 3.0 L; b: 1.5 L) to obtain 16 fractions (1–16). [9]

Fraction 9b (146.3 mg) (eluted with CHCl3, from 0.55 to 0.63 L) was purified by semi-preparative RP HPLC (Symmetry 300 C18 column, 7.8 × 300 mm ID, 7 m particle size (Waters), flow rate of 2.0 mL/min, elution mixture composed of water (A) and CH3OH (B), gradient elution of A:B from 95:5 to 0:100 over 61 min) and afforded 1 (4.3 mg HPLC purity ≥98%).

2.2. Cell cultures

The BC cell lines SKBR-3 and BT474 were obtained from Banca Biologica and Cell Factory in IRCCS Ospedale Policlinico San Martino belonging to the European Culture Collection's Organization. Cells were cultured in DMEM high glucose supplemented with 10% heat-inactivated fetal bovine serum, 1% glutamine, penicillin and streptomycin purchased from Euroclone S.p.A. Control SKBR-3 and BT474 cultures were challenged with DMSO (a suitable solvent for compound 1) at a final concentration of 0.05% and 0.075%, respectively. MCF10A cells were obtained from NIH Institute and cultured according to the manufacturer's instructions.

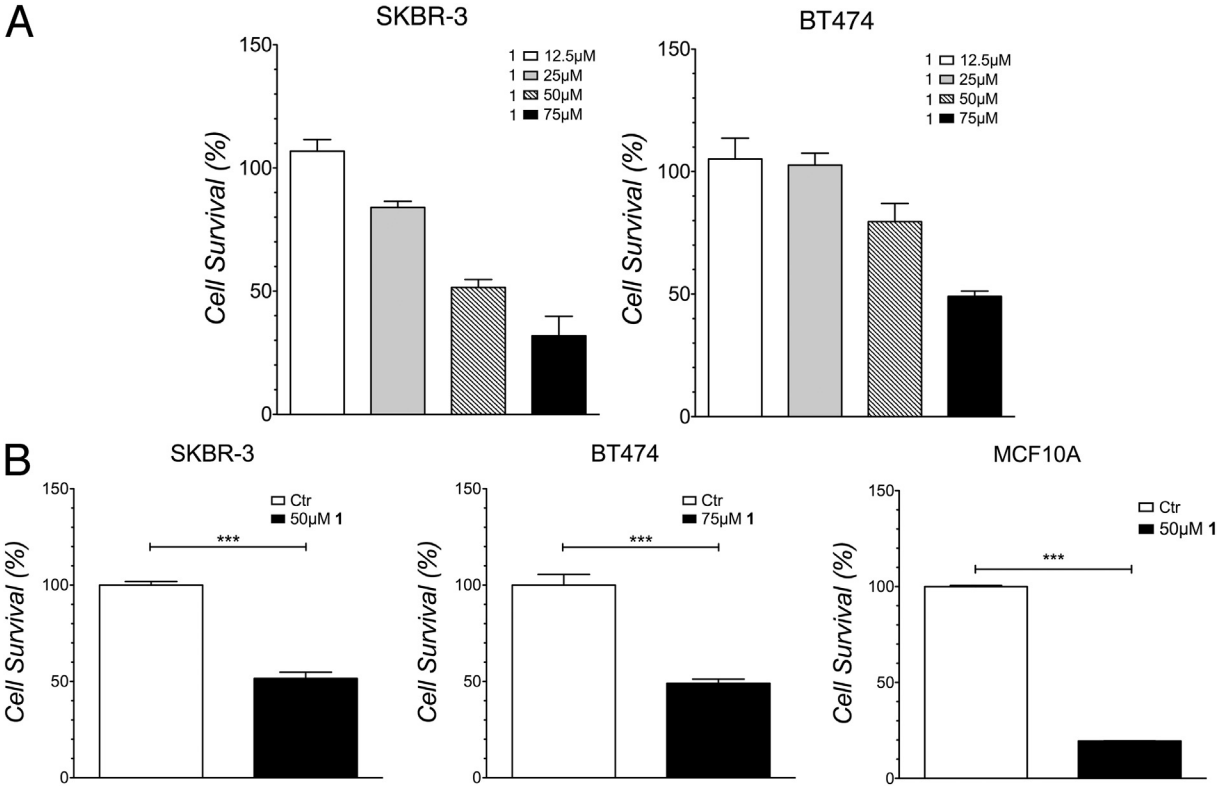

Fig. 2. Compound 1 inhibits cell survival of SKBR-3, BT474 and MCF10A cells. Cells were cultured for 48 h in the presence of DMSO (Control culture, Ctr) or compound 1 at the indicated concentration. Cell survival was assessed by MTT assay. Cell survival in control culture was arbitrarily set to 100%. (A) Compound 1 shows inhibits cell survival of SKBR-3 and BT474 cells in a dose-dependent fashion. (B) Figure shows that 50 μM and 75 μM of compound 1 are concentrations that inhibit at 50% the survival of SKBR-3 and BT474, respectively. Notice that compound 1 at the 50 μM concentration strongly inhibits survival of MCF10A cells. Mean values and standard deviation (indicated as vertical bars) ($n = 4$) are shown. Asterisks indicate statistical significance $P < 0.001$ (***).

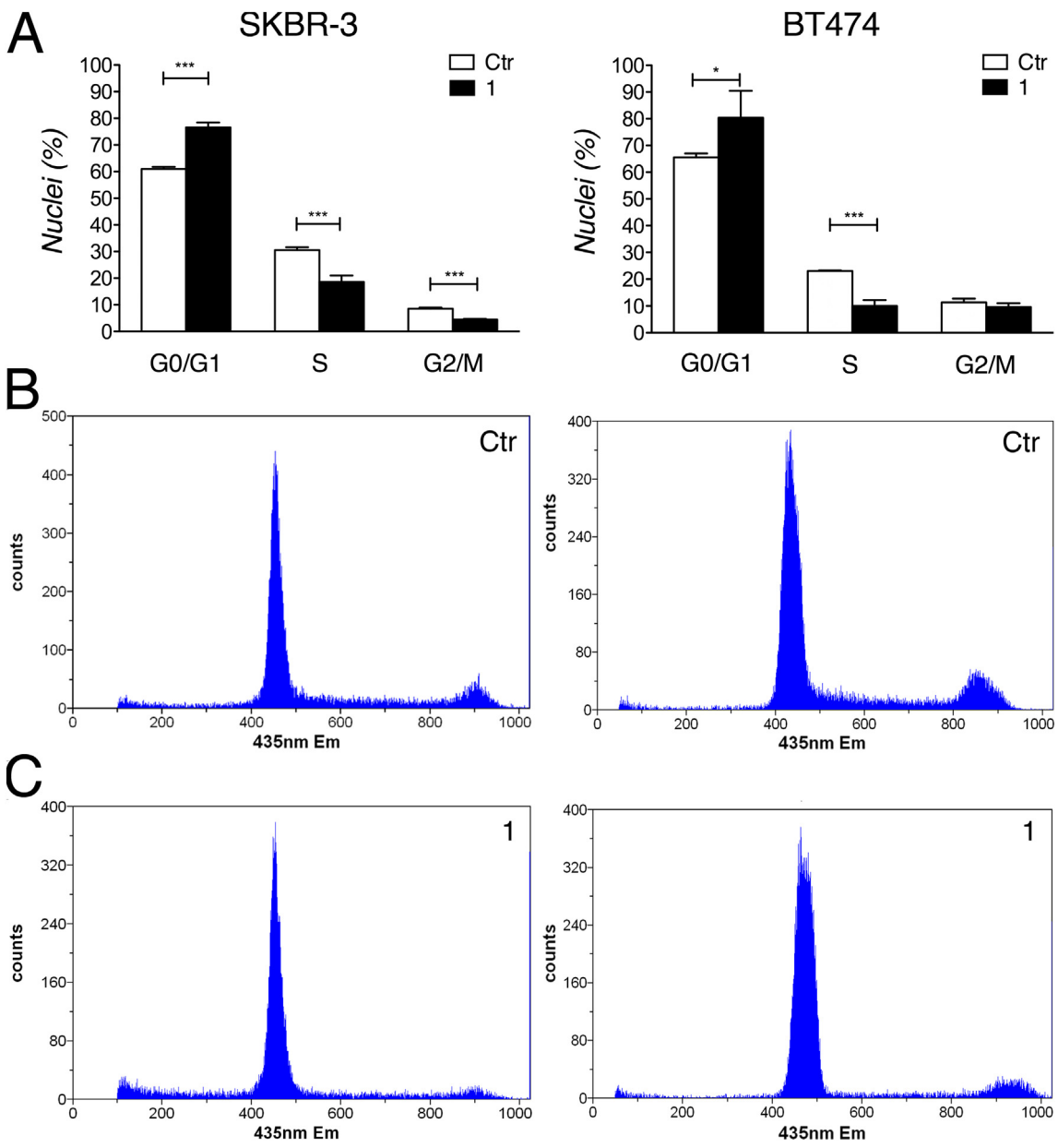

Fig. 3. Compound 1 induces cell cycle arrest of SKBR-3 and BT474 cells in the G0/G1 phase. (A) High resolution DNA flow cytometric analysis of DAPI-stained nuclei of SKBR-3 cells cultured for 48 h with DMSO (Ctr) or 1 supplemented medium. Both floating and adherent cells were collected for the analysis. Mean values and standard deviation (indicated as vertical bars) (n = 4) are shown. P < 0.001 (***).
(B) Representative DNA content histograms obtained by high-resolution DNA flow cytometry from SKBR-3 and BT474 cells treated with DMSO or (C) 1 supplemented medium. X axes show DNA content measured as intensity of fluorescent light emitted by DNA bound DAPI at 435 nm; Y axes show number of nuclei (counts).

2.3. Cell survival assay

Cells were plated in 24-well plates in complete medium (triplicate of SKBR-3 28,000 cells/well, BT474 30,000 cells/well) and compound 1 was administered for 48 h. Cell survival was measured using the 3-(4,5-dimethylthiazol-2yl)-2,5-diphenyltetrazolium bromide (MTT) colorimetric assay.

2.4. Flow cytometry (FCM) analysis

Both adherent and floating cells were collected after 48 h of treatment and centrifuged at 980*g* for 5 min. DNA content in cell nuclei was measured by staining with DAPI and high resolution DNA flow cytometry (hr DNA-FCM) using a Sysmex-Partec CyFlow ML flow cytometer. Cell cycle phases were determined by using the Partec CyFlow software.

Apoptotic and necrotic cells were evaluated by using the Vybrant Apoptosis Assay Kit purchased from Thermo Fisher Scientific with a minor procedure modification as we used the nuclear staining fluorochrome sytox blue instead of the sytox green. Cells were then analyzed using a Beckman Coulter Cyan ADP flow cytometer.

To evaluate ROS generation, we used the cell-permeant ROS probe 2′,7′-dichlorodihydrofluorescein diacetate (H2DCFDA) (also known as dichlorofluorescin diacetate) from Thermo Fisher. After 48 h incubation of the cells with compound 1, we rapidly washed the cells with HBSS and next incubated in HBSS in the presence of 1 μM H2DCFDA for 45 min. Cells were then washed and resuspended in HBSS and immediately analyzed using the Cyan ADP flow cytometer.

To measure mitochondrial membrane potential, we used the fluorescent lipophilic cation dye JC1 purchased from Thermo Fisher

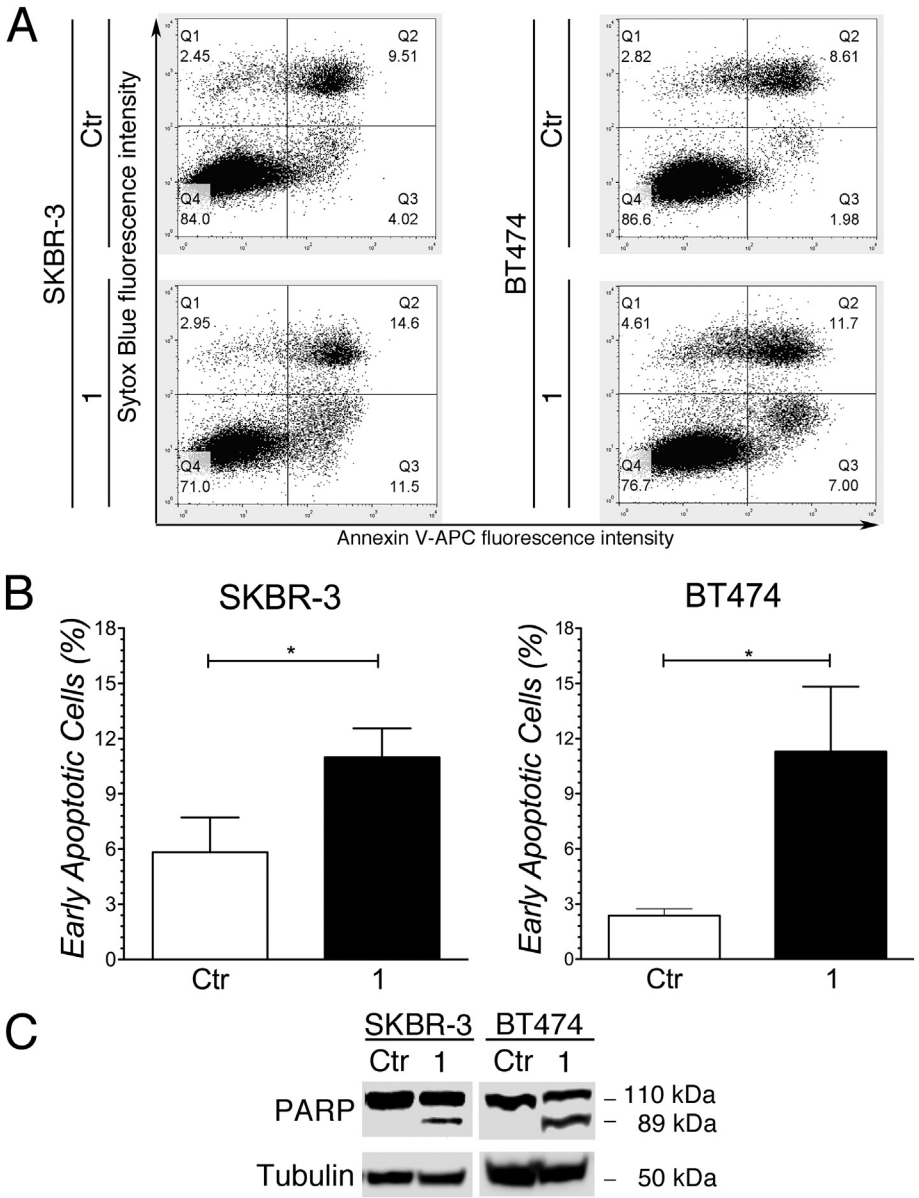

Fig. 4. Compound 1 induces apoptosis in SKBR-3 and BT474 cells. (A) Representative FCM plots of sytox blue and annexin V-APC fluorescence intensity, measured on channel FL6 and FL8, respectively, of SKBR-3 cells (left panels) and BT474 (right panels) after 48 h of exposure to compound 1 (1) or DMSO (Ctr). Both floating and adherent cells were collected for the analysis. Cells analyzed for sytox blue and annexin-APC fluorescence were gated in FCM plots of FSC vs SSC to exclude debris from the analysis (not shown). Percentage of cells included in each quadrant are shown. Early apoptotic cells (sytox blue negative and annexin V-APC positive) are included in the quadrant Q3. (B) The percentage of early apoptotic cells after 48 h of exposure to compound 1 (1) or DMSO (Ctr) is shown. Mean values and SD (indicated as vertical bars) ($n = 3$) are shown. $P < 0.05$ (*). (C) Immunoblot analysis of control (Ctr) or compound 1-treated (1) SKBR-3 and BT474 cell lysates with an antibody against the Poly(ADP-Ribose) Polymerase (PARP). Tubulin was used as a loading control. Molecular masses of the protein bands are indicated in kDa on the right side.

Scientific. Briefly, cells were incubated with 3 μM JC1 for 30 min at 37 °C in a humidified incubator with 5% CO_2 atmosphere, washed with medium twice, and analyzed using a Cyan ADP flow cytometer.

2.5. Immunoblot analysis

SKBR-3 cells were lysed using lysis buffer (Hepes pH 7.4 20 mM, NaCl 150 mM, 10% Glycerol, 1% Triton X-100) containing a protease inhibitors cocktail (Complete) and a phosphatases inhibitor (Phostop) both purchased from Roche Applied Science. Proteins were resolved on SDS-polyacrylamide gel electrophoresis and blotted on a PVDF membrane. Detection was performed with ECL Detection Reagent purchased from BioRad according to manufacturer's protocol. ECL signals were detected and recorded by the Li-Cor scanner and the Nine Aliance, Uvitec Cambridge, gel documentation apparatus. Antibodies against Poly(ADP-Ribose) Polymerase (PARP) and anti-ERK1/2 were purchased from Cell Signaling Technologies Inc. while the anti-tubulin antibody was purchased from Sigma Aldrich. The antibody specific for the ERBB2 N-terminal domain was purchased from Thermo (Ab-20), the anti-phospho-ERK1/2 (Thr 202/Tyr 204) was purchased from Santa Cruz Biotechnology.

2.6. Mitochondrial morphology analysis

To perform epifluorescence analysis, cells were grown on cover slip and mitochondria were stained with 23.5 μM MitoTracker Red CMXRos while nuclei were stained with 5.9 μM Hoechst 33342, both purchased from Thermo Fisher Scientific, for 20 min at 37 °C in a humidified incubator with 5% CO_2 atmosphere. Cells were washed with fresh medium and incubated in medium for further 20 min at 37 °C in incubator. Fixation was performed with PFA 3.7%, 2% sucrose in PBS for 5 min at room temperature. Cells were washed with PBS and mounted on a glass slide. Epifluorescence and real time deconvolution and acquisition was performed with an Zeiss Axio Imager A2M microscope equipped with an Apotome module.

2.7. TEM analysis

For electron microscopy, SKBR-3 cells were seeded on glass chamber slides and treated with compound 1 for 48 h in parallel with control cells. After treatment, cells were washed out in 0.1 M cacodylate buffer and immediately fixed in 0.1 M cacodylate buffer containing 2.5% glutaraldehyde purchased from Electron Microscopy Science, for

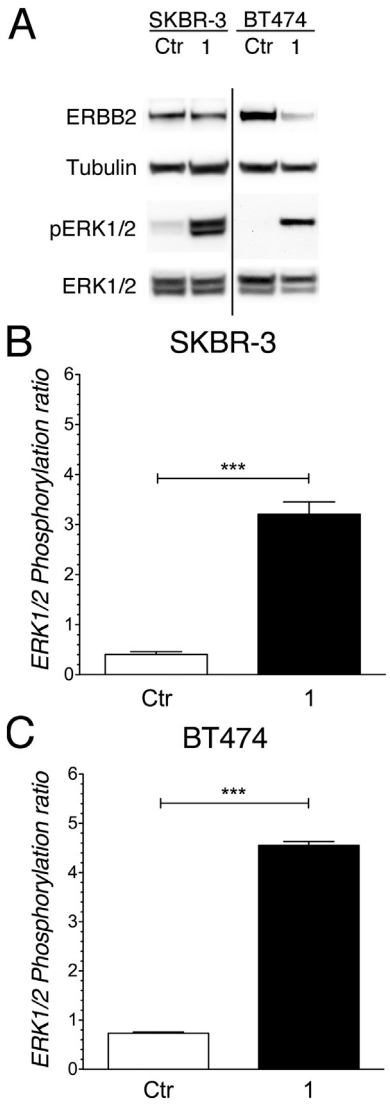

Fig. 5. Compound 1 reduces ERBB2 protein levels and induces ERK1/2 activation in SKBR-3 and BT474 cell lines. (A) Immunoblot analysis of SKBR-3 and BT474 cell lysates after 48 h of exposure to compound 1 (1) or DMSO (Ctr) with antibodies specific for ERBB2 N-terminal domain, ERK1/2 and phosphorylated ERK1/2 isoforms. Tubulin was used as a loading control. Notice that the vertical line indicates that samples were loaded on different gels. (B) ERK phosphorylation was further analyzed using a SureFire ERK assay. Mean pERK1/2 vs total ERK ratio and standard deviation (indicated as vertical bars) ($n = 3$) are shown. $P < 0.001$ (***).

1 h at room temperature. The cells were postfixed in osmium tetroxide for 2 h and 1% uranyl acetate for 1 h. Subsequently, samples were dehydrated through a graded ethanol series and flat embedded in resin Poly-Bed, purchased from Polysciences, for 24 h at 60 °C [10]. Ultrathin sections (50 nm) were cut parallel to the substrate, stained with 5% uranyl acetate in 50% ethanol and observed with a Philips CM10 transmission electron microscope. Digital images were taken with a Megaview 2 CCD camera.

2.8. ATP synthesis assay

ATP synthesis rate was measured by the luciferin/luciferase chemiluminescent method.

2.9. pERK/ERK ratio measurement

Quantification of the pERK/ERK ratio was performed using the Alpha SureFire Ultra Multiplex ERK assay and the EnVision Multilabel Reader both purchased from Perkin-Elmer.

2.10. Statistical analyses

Statistical analyses were performed using the software Prism (GraphPad Software, La Jolla, CA, USA).

All measurements here reported are presented as mean ± standard deviations (SD). For cell survival, apoptosis, mitochondrial membrane potential measure, ATP production, Alphaplex, and ROS production analysis we used a two-tailed distribution Student's *t*-test. For cell cycle phase analysis and cell survival in the presence and absence of NAC, we used one-way ANOVA plus post-hoc Newman-Keuls multiple comparison test. Mean differences were considered statistically significant (*P* value) at $P < 0.05$.

3. Results

3.1. Compound 1 inhibits survival of breast epithelial cells

To investigate whether compound 1 inhibited cell survival as reported for another diterpene with icetexane skeleton *Salvia corrugata* [11,12], we incubated two ERBB2+ BCa cell lines, SKBR-3 and BT474, with this substance for 48 h, then performed an MTT assay. Indeed, we found that compound 1 inhibited in a concentration-dependent manner the survival of these cells (Fig. 2A). In particular, the compound 1 concentration that showed 50% inhibition of survival after 48 h of treatment compared to controls (IC_{50}) were 50 μM and 75 μM for SKBR-3 and BT474, respectively (Fig. 2B). These IC_{50} concentrations and a treatment of 48 h were used for all subsequent experiments with SKBR-3 and BT474. Control SKBR-3 and BT474 cultures were challenged with DMSO (a suitable solvent for compound 1) at a final concentration of 0.05% and 0.075%, respectively.

To assess whether compound 1 was active against normal breast epithelial cells, we choose to use the MCF10A cell line that, although immortalized, are considered an acceptable model for normal human breast epithelial cells. We treated these cells for 48 h with the lowest concentration of compound 1 used for BCa cells (50 μM) and performed an MTT assay. Control MFC10A cultures were treated with DMSO at a final concentration of 0.05%. Fig. 2B shows that compound 1 indeed dramatically inhibited MCF10A survival.

3.2. Compound 1 causes a cell cycle arrest in G0/G1 and apoptosis of ERBB2+ BCa cells

To investigate whether a cell cycle progression arrest contributed to the observed inhibition of cell survival, we evaluated the DNA content of cell nuclei by hr DNA-FCM. This analysis showed that compound 1 increased the percentage of cells in the G0/G1 phases compared to control cultures. This arrest in G0/G1 was accompanied by a reduction of the percentage of cells in the S phase in both SKBR-3 and BT474 (Fig. 3A–C). To establish whether the anti-proliferative effect of compound 1 was accompanied by apoptosis in $ERBB2^+$ BCa cells, we performed an apoptosis assay. This assay allowed us to identify early apoptotic, late apoptotic, and necrotic cells. Representative FCM plots used to perform apoptosis analysis are provided in Fig. 4A. In particular, we found a higher number of early apoptotic cells in cultures of both cell lines treated with compound 1 compared to control cultures ($P < 0.05$) (Fig. 4B). No statistically significantly differences were observed in the number of late apoptotic or necrotic cells between treated and control cultures (data not shown). Furthermore, immunoblot analysis of cell lysates showed cleavage of the Poly(ADP-Ribose) Polymerase (PARP) in cells treated with compound 1 but not in

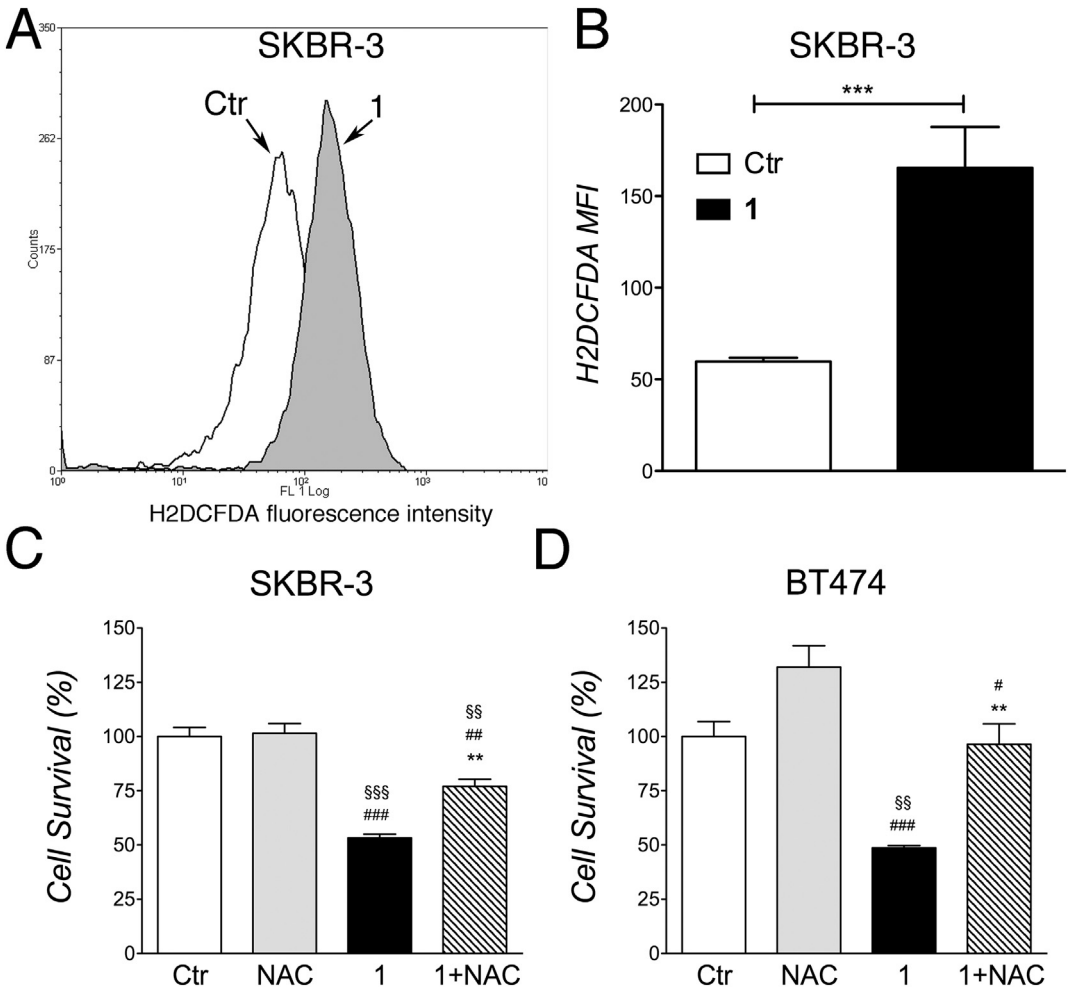

Fig. 6. Compound 1 induces ROS generation in SKBR-3 cells and survival of SKBR-3 and BT474 cells is enhanced by NAC. (A). Representative FCM plot of FL1 intensity vs. counts of SKBR-3 cells stained with H2DCFDA to measure ROS generation after 48 h of exposure to compound 1 (1) or DMSO (Ctr). Cells analyzed for H2DCFDA fluorescence were gated in FCM plots of FSC vs SSC to exclude debris from the analysis (not shown). (B) H2DCFDA mean fluorescence intensity (MFI) of cells stained after 48 h of exposure to compound 1 (1) or DMSO (Ctr). Mean values and standard deviation (indicated as vertical bars) ($n = 4$) are shown. $P < 0.001$ (***). (C, D) SKBR-3 and BT474 cells were cultured for 48 h in the presence of DMSO (Ctr) or compound 1 (1) or NAC 4 mM, or both 1 and NAC. Cell survival was assessed by MTT assay. Cell survival in control culture was arbitrarily set to 100%. Mean values and standard errors of the mean (indicated as vertical bars) (n = 4) are shown. $P < 0.05$ ($^{\#}$), $P < 0.01$ ($^{**,\S\S,\#\#}$), $P < 0.001$ ($^{\S\S\S,\#\#\#}$). Statistical significance of 1 and 1 + NAC vs. Ctr is indicated by §. Statistical significance of 1 and 1 + NAC vs. NAC is indicated by $^{\#}$. Statistical significance of 1 + NAC versus 1 is indicated by *.

controls (Fig. 4C), which confirmed apoptosis induced by compound 1.

3.3. Compound 1 modulates ERBB2 signaling

As ERBB2 and its downstream signaling which includes ERK1/2 modulation are key elements for ERBB2 BCa cells survival, we investigated whether compound 1 affected ERBB2 and pERK1/2 levels by immunoblot analysis. This analysis showed a minor reduction of ERBB2 levels in SKBR-3 and a major one in BT474 cells (Fig. 5A). In contrast, we observed a dramatic increase in ERK1/2 phosphorylation in both cell types (Fig. 5A). To better evaluate this increase we employed an assay able to detect simultaneously in cell lysates both total and phosphorylated ERK1/2 protein levels. The results showed that the ratio of the phosphorylated vs. total ERK1/2 levels were about 7-fold higher in both SKBR-3 (Fig. 5B) and BT474 (Fig. 5C) compound 1-treated cultures compared with controls ($P < 0.001$). This indicated that compound 1 promoted activation of ERK1/2.

3.4. Compound 1 causes ROS stress

Because reactive oxygen species have been found to promote ERK activation [13], we decided to test whether compound 1 treated ERBB2 cells displayed generation of ROS. We labelled SKBR3 cells with the ROS probe H2DCFDA in the presence and absence of compound 1 and measured by FCM the median fluorescent intensity (MFI). A representative plot of this FCM analysis is shown in Fig. 6A. The results showed a statistically significant ($p < 0.001$) higher MFI in compound 1 treated cells compared to control cells (Fig. 6B).

To demonstrate that compound 1 is responsible of the cell survival inhibition via ROS generation, we treated both cell lines with compound 1 in the presence of *n*-acetylcysteine (NAC), a well-known antioxidant agent. We found in both SKBR-3 and BT474 a statistically significant ($P < 0.01$) increase in survival between cells treated with both compounds compared to compound 1 alone (Fig. 6B, C). Overall, our results strongly suggested that a ROS mediated mechanism contributes to the proapoptotic and anti-survival activities of compound 1 in ERBB2+ BCa cell lines.

3.5. Compound 1 causes mitochondrial damage

It has been reported that activation of ERK1/2 can induce cell death under oxidative stress leading to mitochondria damage [14]. For

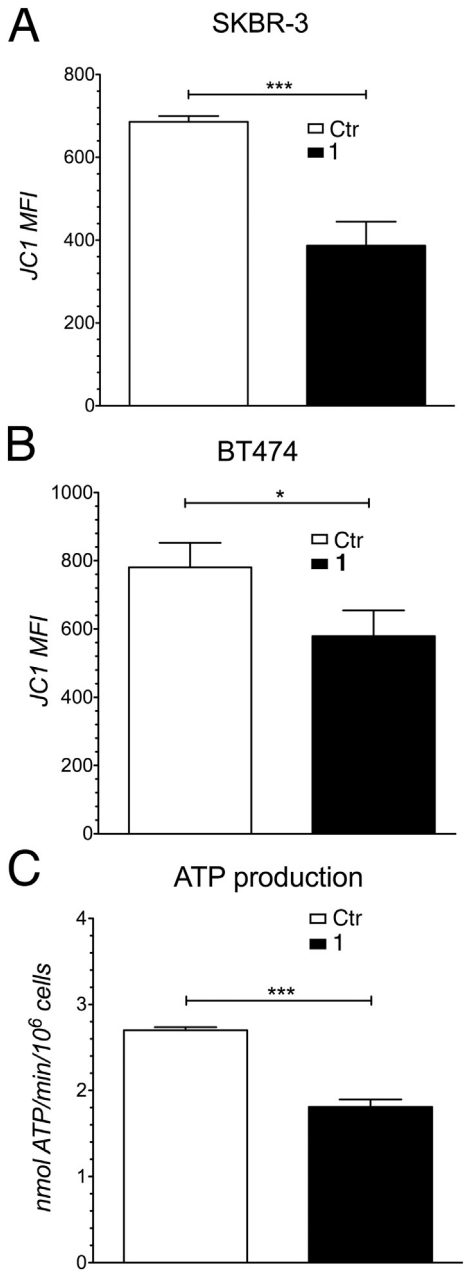

Fig. 7. Compound 1 reduces mitochondrial protonic gradient in SKBR-3 and BT474 and impairs ATP production in SKBR-3 cells. (A, B) Mitochondrial protonic gradient was measured by FCM analysis using the FL2 mean fluorescence intensity (MFI) of SKBR-3 and BT474 cells stained with JC1 after 48 h of exposure to compound 1 (1) or DMSO (Ctr). Mean values and SD (indicated as vertical bars) (n = 3) are shown. P < 0.001 (***). (C) ATP synthesis rate was measured by a luciferin/luciferase chemiluminescent method in SKBR-3 cells treated for 48 h with DMSO (Ctr) or compound 1 (1). Mean values and SD (indicated as vertical bars) (n = 3) are shown. P < 0.001 (***).

example, Ras-Raf-MEK-dependent oxidative cell death is associated with the activation of mitochondrial voltage-dependent anion channels (VDACs) in non-neuronal cells [14], suggesting that mitochondrial membrane potential alterations may play an important role in MAPK-dependent cell death. Signs of mitochondrial dysfunction, which include mitochondrial fragmentation, decreased mitochondrial membrane potential (MMP), diminished ATP production and increased generation of reactive oxygen species (ROS) has been related to apoptosis [15]. Furthermore, we previously observed that the diterpenoid demethyl fruticulin A (SCO-1), extracted from *Salvia corrugata* [16], impairs mitochondrial function [11]. Therefore, we sought to establish whether compound 1 has inhibitory effects on this organelle as well. First, we evaluated the mitochondrial membrane potential (MMP) in SKBR-3 by using a FCM based assay and the cationic fluorochrome JC1. Our analysis showed that compound 1 significantly reduced the mitochondrial membrane potential compared to controls (Fig. 7A, B). Second, we performed an ATP production assay in SKBR-3 cells to establish whether the reduction in the MMP translated in an impairment of ATP synthesis. As expected, our results showed that compound 1-treated cells generated indeed less ATP than control cells ($P < 0.001$) (Fig. 7C).

To characterize the effects of compound 1 on mitochondria morphology, we performed an epifluorescence microscopy analysis with the MitoTracker Red CMXRos fluorochrome in SKBR-3 cells. In control cells, we promptly detected an extended mitochondrial network (Fig. 8A) whereas in compound 1-treated cells the mitochondrial network was collapsed (Fig. 8B). In particular, the MitoTracker Red CMXRos stained a compact perinuclear region where individual mitochondrial filaments were difficult to identify. Furthermore, cells displaying several donut-shaped mitochondria were frequently observed in compound 1-treated cultures (Fig. 8B), while they were only an occasional finding in control cells (not shown). Aberrant morphology of mitochondrial network would reflect alterations of their internal ultrastructure. We performed TEM analysis on SKBR3 cells and we observed distinct types of mitochondrial abnormalities upon treatment with compound 1 (Fig. 8C–F). In particular, we noted alterations and remodeling of inner cristae membranes, which are a common finding during stress and/or apoptosis. Compound 1–treated mitochondria mostly exhibit reduced and swollen cristae (Fig. 8D), which resemble the donut-shaped mitochondria observed by epifluorescence (Fig. 8B). In addition, several mitochondria show a completely disorganized inner membrane topology and occasionally, some mitochondria show small round inclusions in the mitochondrial matrix (Fig. 8E, F) and discontinuity of the outer membrane (Fig. 8F).

4. Discussion

The *ERBB2* gene is amplified or overexpressed in approximately 30% of human breast cancers and in many other cancer types [10,17–19]. The advent of ERBB2-directed therapies has significantly improved the overall survival for patients with ERBB2$^+$ early stage breast cancers. Nowadays, cancer chemoprevention and treatment using natural phytochemicals is emerging as an attractive and safer strategy in addition to conventional therapies. Because of the innate or acquired resistance of ERBB2$^+$ breast cancers to currently available targeted agents, we performed the present in vitro study to assess the therapeutic potential of compound 1 by evaluating its effects on ERBB2$^+$ cell growth and survival as well as ERBB2 downstream signaling.

We have shown that compound 1 exerted a concentration-dependent growth inhibition in SKBR3 and BT474 ERBB2$^+$ cell lines. In particular, we found that 1 induced a block of the cell cycle in the G0/G1 phase along with a reduction of the percentage of cells in the S and G2/M phases. Furthermore, compound 1 induced apoptosis as shown by a higher fraction of early apoptotic cells and PARP cleavage found in 1-treated cultures compared to controls. Overall, these results indicate striking anti-proliferative and proapoptotic activities for 1. Unfortunately, we found that 1 was also effective in inhibiting the growth of the MCF10A non transformed human mammary cells, thus limiting its potential therapeutic use. However, although this cell line is widely used as normal counterpart of breast cancer cell lines it should be considered that it is an immortalized line. Therefore, the effects of compound 1 on normal cells should be further investigated in future studies. Furthermore, as to our knowledge this is the first study on this compound, we cannot rule out that it may induce cell death at lower concentrations in other cancer cell types.

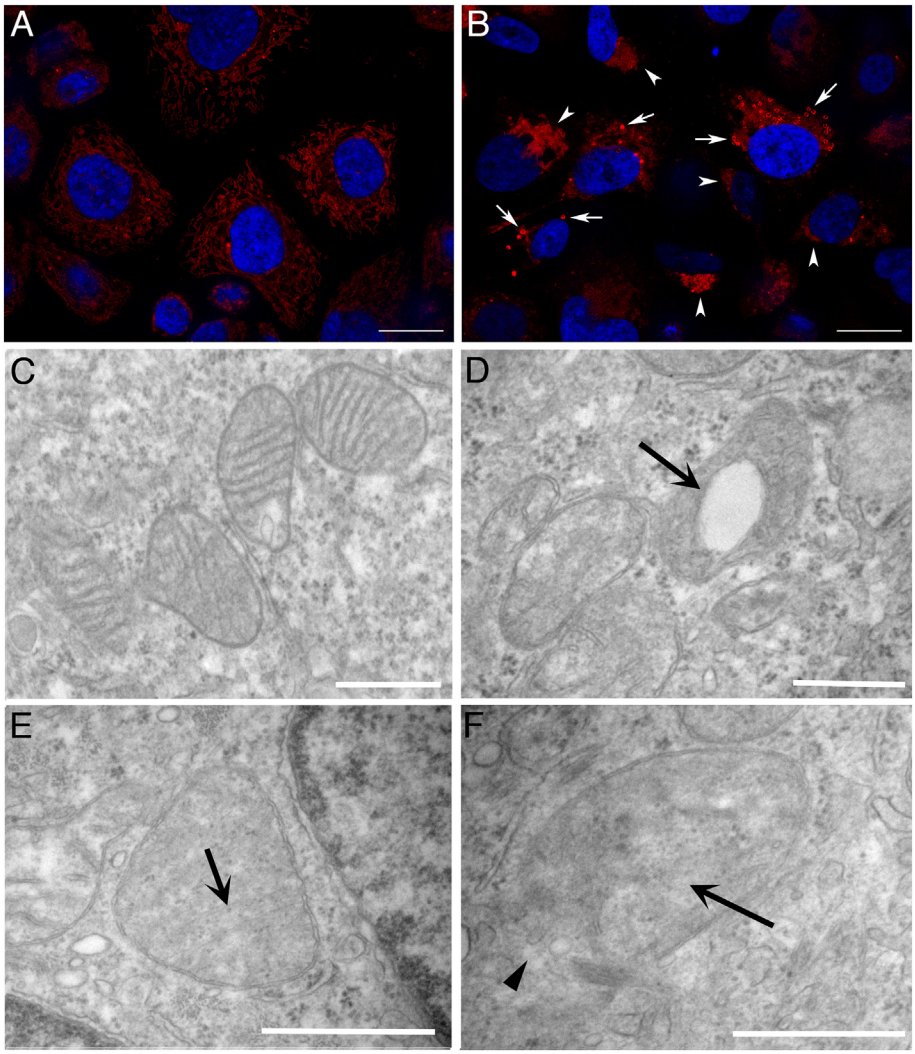

Fig. 8. Compound 1 causes mitochondrial network collapse and donuts formation. Mitochondria of SKBR-3 cells were stained by using MitoTracker Red CMXRos (red signal), whereas nuclei were stained with Hoechst 33342 (blue signal) after 48 h of exposure to compound 1 (A) or DMSO (B). Arrows indicates mitochondrial network collapse, arrowheads indicate some donut-shaped mitochondria. Bar = 64.5 μm. Compound 1 causes mitochondrial network remodeling of inner cristae membranes and discontinuity of the outer membrane in SKBR-3 cells. Ultrastructural analysis of mitochondria in untreated (C) and treated cells with compound 1 for 48 h (D–F). Representative TEM images showing mitochondria with alterations and remodeling of inner cristae membranes (D, E, arrows). Several mitochondria show a completely disorganized inner membrane topology (F, arrow) and discontinuity of the outer membrane (F, arrowhead). Scale bar: 500 nm. (For interpretation of the references to color in this figure legend, the reader is referred to the web version of this article.)

Concerning the ERBB2 signaling, we investigated whether compound 1 affected ERBB2 protein levels and both ERK1/2 activation and protein levels as downstream effector. We found that compound 1 effect on ERBB2 may be cell context dependent as it strongly down-regulated ERBB2 in BT474, while only a minor decrease was observed in SKBR-3 cells. On the contrary, compound 1 strikingly enhanced ERK1/2 activation in both cell types, while ERK1/2 protein levels were unaffected. A number of studies show that ERK1/2 has a pro-apoptotic role depending from the stimulus, cell type and downstream effectors activated [20]. As corroborating findings, apoptosis via ERK1/2 activation has been demonstrated for triterpenes such as asiatic acid [21] and euphol [22]. Therefore, we suggest that compound 1 engages the apoptotic program via activation of ERK1/2 kinase.

It has been reported that activation of ERK1/2 can induce cell death under oxidative stress leading to mitochondria damage. For example, Ras-Raf-MEK-dependent oxidative cell death is associated with the activation of mitochondrial voltage-dependent anion channels (VDACs) in non-neuronal cells [14], suggesting that mitochondrial membrane potential alterations may play an important role in MAPK-dependent cell death. Signs of mitochondrial dysfunction, which include mitochondrial fragmentation, decreased mitochondrial membrane potential (MMP), diminished ATP production and increased generation of reactive oxygen species (ROS) has been related to apoptosis [15]. Consistently, we found that compound 1 strongly inhibited MMP and ATP production in both BC cell lines. As expected, dramatic changes in the mitochondrial network morphology were occurring upon 1 administration to BCa cells, as demonstrated by epifluorescence. Mitochondria often appeared collapsed and donut-shaped upon compound 1 treatment. At the ultrastructural level, we observed disarrangement and distortion of inner cristae membranes, which resembled the donut-shaped mitochondria observed by epifluorescence, and that are common during stress and/or apoptosis. Some mitochondria showed small round inclusions in the mitochondrial matrix and others showed discontinuity in the outer membrane. We hypothesize that 1-mediated ERK1/2 activation in ERBB2$^+$ BC cells is associated with MAPK-dependent cell death through ROS production and mitochondrial collapse, which eventually lead to apoptosis. In support to this hypothesis, we showed that the anti-oxidant NAC rescued cell survival of cells treated with compound 1. Therefore, we propose a model in which compound 1-mediated ROS production and ERK1/2 activation is associated with MAPK-dependent cell death through mitochondrial collapse.

In conclusion, we have shown that compound 1 exerts its antiproliferative and killing effects by blocking the cell cycle in G0/G1 phase and by apoptosis activation, through ROS generation, mitochondrial dysfunction and collapse. However, this compound fails to exhibit clinical potential in ERBB2$^+$ cancer due to requirement of rather high-doses to inhibit cell survival in vitro and lack of specificity towards breast cancer cells. However, further research could lead to the development of compound 1 analogues with improved activity and specificity, which might contribute to cancer prevention.

Funding sources

This research did not receive any specific grant from funding agencies in the public, commercial, or not-for-profit sectors.

Declaration of Competing Interest

The authors declare no conflict of interest.

References

[1] D.J. Lobbezoo, R.J. van Kampen, A.C. Voogd, M.W. Dercksen, F. van den Berkmortel, T.J. Smilde, A.J. van de Wouw, F.P. Peters, J.M. van Riel, N.A. Peters, et al., Prognosis of metastatic breast cancer: are there differences between patients with de novo and recurrent metastatic breast cancer? Br. J. Cancer 112 (9) (2015) 1445–1451.

[2] X. Dai, T. Li, Z. Bai, Y. Yang, X. Liu, J. Zhan, B. Shi, Breast cancer intrinsic subtype classification, clinical use and future trends, Am. J. Cancer Res. 5 (10) (2015) 2929–2943.

[3] O. Yersal, S. Barutca, Biological subtypes of breast cancer: prognostic and therapeutic implications, World J Clin Oncol 5 (3) (2014) 412–424.

[4] A. Daemen, G. Manning, HER2 is not a cancer subtype but rather a pan-cancer event and is highly enriched in AR-driven breast tumors, Breast Cancer Res. 20 (1) (2018) 8.

[5] E.Y. Ko, A. Moon, Natural products for chemoprevention of breast cancer, J Cancer Prev 20 (4) (2015) 223–231.

[6] M. Gonzalez-Vallinas, G. Reglero, A. Ramirez de Molina, Rosemary (Rosmarinus officinalis L.) extract as a potential complementary agent in anticancer therapy, Nutr. Cancer 67 (8) (2015) 1221–1229.

[7] K. Cortese, A. Daga, M. Monticone, S. Tavella, A. Stefanelli, C. Aiello, A. Bisio, G. Bellese, P. Castagnola, Carnosic acid induces proteasomal degradation of cyclin B1, RB and SOX2 along with cell growth arrest and apoptosis in GBM cells, Phytomedicine 23 (7) (2016) 679–685.

[8] C. D'Alesio, G. Bellese, M.C. Gagliani, C. Aiello, E. Grasselli, G. Marcocci, A. Bisio, S. Tavella, T. Daniele, K. Cortese, et al., Cooperative antitumor activities of carnosic acid and trastuzumab in ERBB2(+) breast cancer cells, J. Exp. Clin. Cancer Res. 36 (1) (2017) 154.

[9] A. Bisio, D. Fraternale, A.M. Schito, A. Parricchi, F. Dal Piaz, D. Ricci, M. Giacomini, B. Ruffoni, N. De Tommasi, Establishment and analysis of in vitro biomass from Salvia corrugata Vahl. and evaluation of antimicrobial activity, Phytochemistry 122 (2016) 276–285.

[10] M. Minuto, E. Varaldo, G. Marcocci, A. de Santanna, E. Ciccone, K. Cortese, ERBB1- and ERBB2-positive medullary thyroid carcinoma: a case report, Diseases 6 (2) (2018).

[11] M. Monticone, A. Bisio, A. Daga, P. Giannoni, W. Giaretti, M. Maffei, U. Pfeffer, F. Romeo, R. Quarto, G. Romussi, et al., Demethyl fruticulin A (SCO-1) causes apoptosis by inducing reactive oxygen species in mitochondria, J. Cell. Biochem. 111 (5) (2010) 1149–1159.

[12] P. Giannoni, R. Narcisi, D. De Totero, G. Romussi, R. Quarto, A. Bisio, The administration of demethyl fruticulin A from Salvia corrugata to mammalian cells lines induces “anoikis”, a special form of apoptosis, Phytomedicine 17 (6) (2010) 449–456.

[13] S. Cagnol, J.C. Chambard, ERK and cell death: mechanisms of ERK-induced cell death—apoptosis, autophagy and senescence, FEBS J. 277 (1) (2010) 2–21.

[14] N. Yagoda, M. von Rechenberg, E. Zaganjor, A.J. Bauer, W.S. Yang, D.J. Fridman, A.J. Wolpaw, I. Smukste, J.M. Peltier, J.J. Boniface, et al., RAS-RAF-MEK-dependent oxidative cell death involving voltage-dependent anion channels, Nature 447 (7146) (2007) 864–868.

[15] J.P. Wang, C.H. Hsieh, C.Y. Liu, K.H. Lin, P.T. Wu, K.M. Chen, K. Fang, Reactive oxygen species-driven mitochondrial injury induces apoptosis by teroxirone in human non-small cell lung cancer cells, Oncol. Lett. 14 (3) (2017) 3503–3509.

[16] A. Bisio, G. Romussi, E. Russo, S. Cafaggi, A.M. Schito, B. Repetto, N. De Tommasi, Antimicrobial activity of the ornamental species Salvia corrugata, a potential new crop for extractive purposes, J. Agric. Food Chem. 56 (22) (2008) 10468–10472.

[17] J.S. Ross, M. Fakih, S.M. Ali, J.A. Elvin, A.B. Schrock, J. Suh, J.A. Vergilio, S. Ramkissoon, E. Severson, S. Daniel, et al., Targeting HER2 in colorectal cancer: the landscape of amplification and short variant mutations in ERBB2 and ERBB3, Cancer 124 (7) (2018) 1358–1373.

[18] W. Shibata, H. Kinoshita, Y. Hikiba, T. Sato, Y. Ishii, S. Sue, M. Sugimori, N. Suzuki, K. Sakitani, H. Ijichi, et al., Overexpression of HER2 in the pancreas promotes development of intraductal papillary mucinous neoplasms in mice, Sci. Rep. 8 (1) (2018) 6150.

[19] P. Castagnola, G. Bellese, F. Birocchi, M.C. Gagliani, C. Tacchetti, K. Cortese, Identification of an HSP90 modulated multi-step process for ERBB2 degradation in breast cancer cells, Oncotarget 7 (51) (2016) 85411–85429.

[20] Y. Mebratu, Y. Tesfaigzi, How ERK1/2 activation controls cell proliferation and cell death: is subcellular localization the answer? Cell Cycle 8 (8) (2009) 1168–1175.

[21] Y.L. Hsu, P.L. Kuo, L.T. Lin, C.C. Lin, Asiatic acid, a triterpene, induces apoptosis and cell cycle arrest through activation of extracellular signal-regulated kinase and p38 mitogen-activated protein kinase pathways in human breast cancer cells, J. Pharmacol. Exp. Ther. 313 (1) (2005) 333–344.

[22] M.W. Lin, A.S. Lin, D.C. Wu, S.S. Wang, F.R. Chang, Y.C. Wu, Y.B. Huang, Euphol from Euphorbia tirucalli selectively inhibits human gastric cancer cell growth through the induction of ERK1/2-mediated apoptosis, Food Chem. Toxicol. 50 (12) (2012) 4333–4339.